Published in final edited form as:
Bioconjug Chem. 2009 April ; 20(4): 790–798. doi:10.1021/bc800545e.

Evaluation of ^{64}Cu(DO3A-xy-TPEP) as A Potential PET Radiotracer for Monitoring Tumor Multidrug Resistance

Shuang Liu*, **Young-Seung Kim**, **Shizhen Zhai**, **Jiyun Shi**, and **Guihua Hou**
School of Health Sciences, Purdue University, West Lafayette, Indiana

Abstract

In this study, we evaluated the potential of ^{64}Cu(DO3A-xy-TPEP) (DO3A-xy-TPEP = (2-(diphenylphosphoryl)ethyl)diphenyl(4-((4,7,10-tris(carboxymethyl)-1,4,7,10-tetraazacyclododecan-1-yl)methyl)benzyl)phosphonium) as a PET (positron emission tomography) radiotracer for noninvasive monitoring of multidrug resistance (MDR) transport function in several xenografted tumor models (MDR-negative: U87MG; MDR-positive: MDA-MB-435, MDA-MB-231, KB-3-1 and KB-v-1). It was found that ^{64}Cu(DO3A-xy-TPEP) has a high initial tumor uptake (5.27 ± 1.2 %ID/g at 5 min p.i.) and show a steady uptake increase between 30 and 120 min p.i. (2.09 ± 0.53 and 3.35 ± 1.27 %ID/g at 30 and 120 min p.i., respectively) in the MDR-negative U87MG glioma tumors. ^{64}Cu(DO3A-xy-TPEP) has a greater uptake difference between U87MG glioma and MDR-positive tumors (MDA-MB-231: 1.57 ± 0.04, 1.00 ± 0.17, and 0.93 ± 0.15; MDA-MB-435: 1.15 ± 0.19, 1.12 ± 0.20, and 0.81 ± 0.11; KB-3-1: 1.45 ± 0.31, 1.43 ± 0.16, and 1.08 ± 0.19; and KB-v-1: 1.63 ± 0.47, 1.81 ± 0.31, and 1.14 ± 0.22 %ID/g at 30, 60 and 120 min p.i., respectively) than ^{99m}Tc-Sestamibi. Regardless of the source of MDR, the overall net effect is the rapid efflux of ^{64}Cu(DO3A-xy-TPEP) from tumor cells, which leads to a significant reduction of its tumor uptake. It was concluded that ^{64}Cu(DO3A-xy-TPEP) is more efficient than ^{99m}Tc-Sestamibi as the substrate for MDR P-glycoproteins (MDR Pgps) and multidrug resistance-associated proteins (MRPs), and might be a more efficient radiotracer for noninvasive monitoring of the tumor MDR transport function. ^{64}Cu(DO3A-xy-TPEP) and ^{99m}Tc-Sestamibi share almost identical subcellular distribution patterns in U87MG glioma tumors. Thus, it is reasonable to believe that ^{64}Cu(DO3A-xy-TPEP), like ^{99m}Tc-Sestamibi, is able to localize in mitochondria due to the increased plasma and mitochondrial transmembrane potentials in tumor cells.

Keywords

^{64}Cu radiotracers; PET imaging; tumor multidrug resistance

INTRODUCTION

Cancer is the second leading cause of death world wide. The most prevalent forms of the disease are solid tumors of the lung, breast, prostate, colon and rectum. Although the exact cause of cancer remains unknown, most cancer patients will survive after surgery, radiation therapy, and chemotherapy or a combination thereof if it can be detected at the early stage. Therefore, accurate early detection is highly desirable so that various therapeutic regiments can be given before the tumors become widely spread.

*To whom correspondence should be addressed. School of Health Sciences, Purdue University, 550 Stadium Mall Drive, West Lafayette, IN 47907. Phone: 765-494-0236; Fax 765-496-1377; Email: E-mail: lius@pharmacy.purdue.edu.

Multidrug resistance (MDR) remains a major obstacle in the treatment of cancer. The over-expression of multidrug resistance P-glycoproteins (MDR Pgps) and multidrug resistance-associated proteins (MRPs) in tumor cells has been shown to confer MDR onto drug-sensitive cells (1–3). Both MDR Pgps and MRPs belong to a large family of ATP-trafficking proteins that mediate the transport of a large number of drug molecules (3–6). Although the molecular mechanism is not entirely clear, the net effect of MDR Pgp and MRP overexpression is the reduced intracellular drug accumulation through an energy-dependent drug efflux in the MDR-positive cancer cells as compared with the drug-sensitive tumor cells (5,6). While several different genes are associated with the MDR phenotype (6,7), the MDR mediated by overexpression of MDR1 Pgp is one of the best characterized barriers to chemotherapeutics treatment. High levels of MDR1 Pgp expression has been detected in more than 50% of tumors (8–11). A correlation between the MDR1 Pgp expression and failure of chemotherapy or poor survival rates has been established (11). However, the lack of MDR1 Pgp in other MDR-positive tumors indicates that additional cellular changes also confer resistance to anticancer drugs (12–15). For example, MRP1 expression in retinoblastoma correlated well with the rare failure of chemotherapy (16). The lung resistance protein (LRP) and breast cancer resistance protein (BCRP) have also been observed in tumor cells (17,18). More recently, the overexpression of a 40 kDa protein (P-40 or Annexin I) was reported in tumor cell lines w/o MDR1 Pgp (19,20). Since MDR is a major obstacle in chemotherapy of cancer patients, there has been a continuing demand for radiotracers that are able to monitor the tumor MDR transport function in a noninvasive fashion (21–27).

Cationic radiotracers, such as ^{99m}Tc-Sestamibi and ^{99m}Tc-Tetrofosmin, tend to localize in tumor cells due to the increased negative mitochondrial potentials (28–35). ^{99m}Tc-Sestamibi and ^{99m}Tc-Tetrofosmin have been clinically used for both cancer early detection and non-invasive monitoring of the tumor MDR transport function by single photon emission computed tomography (SPECT) (21–27,30). However, their diagnostic and prognostic values are often limited due to their insufficient tumor localization and high uptake in the heart, liver and muscle, which makes it very difficult to detect small lesions in the chest and abdominal regions. Thus, there is an unmet medical need for the radiotracers that are able to monitor noninvasively the MDR transport function in tumors.

Previously, we reported ^{64}Cu-labeled organic phosphonium cations, such as ^{64}Cu(DO3A-xy-TPEP) (Figure 1: DO3A-xy-TPEP = (2-(diphenylphosphoryl)ethyl)diphenyl(4-((4,7,10-tris (carboxymethyl)-1,4,7,10-tetraazacyclododecan-1-yl)methyl)benzyl)phosphonium), as a potential PET (positron emission tomography) radiotracer in the athymic nude mice bearing U87MG human glioma xenografts (36–39). Both biodistribution and in vivo microPET imaging studies demonstrated that ^{64}Cu(DO3A-xy-TPEP) has higher tumor uptake with better tumor selectivity (as defined by their tumor/heart and tumor/muscle ratios) than ^{99m}Tc-Sestamibi (Figure 1). These promising results lead us to explore the potential of ^{64}Cu(DO3A-xy-TPEP) as a PET radiotracer for noninvasive monitoring of the MDR transport function in athymic nude mice bearing MDR-positive tumor xenografts.

The tumor cell lines used in this study include U87MG human glioma, MDA-MB-231 and MDA-MB-435 human breast cancer, KB-3-1 and KB-v-1. The U87MG glioma cell line was chosen because it has no over-expression of MDR1 Pgp (40–42). The U87MG cell line has been used for evaluation of the cellular uptake kinetics of ^{99m}Tc-Sestamibi and ^{99m}Tc-Tetrofosmin (43). MDA-MB-435 is the estrogen-independent human breast cancer cell line (metastatic ductal adenocarcinoma), and has a low level of MDR1 expression (44–47) and a high level expression of MRP2 and MRP4 (47,48). MDA-MB-231 is also an estrogen-independent human breast cancer cell line, and is often considered “drug-sensitive” because it has little MDR1, MRP1 and BCRP overexpression (47,48). However, recent studies have clearly demonstrated that the MDA-MB-231 breast tumor cell line has a high level expression

of P-40, a 40 kDa protein (19,20). The athymic nude mice bearing KB-3-1 and KB-v-1 tumor xenografts have been successfully used to evaluate cationic ^{99m}Tc and ^{68}Ga radiotracers (49–56), as well as luminescent probes (57). High level expression of MDR Pgps or/and MRPs will result in a rapid efflux of the cationic radiotracer from tumor cells and the significant reduction in tumor localization of the radiotracer. Since it has been used for imaging the tumor MDR transport function by SPECT (21–27), ^{99m}Tc-Sestamibi was as the "control". We are interested in ^{64}Cu(DO3A-xy-TPEP) due its high tumor uptake and rapid liver clearance in nude mice bearing the MDR-negative U87MG human glioma xenografts (39). The main objective of this study is to evaluate the potential of ^{64}Cu(DO3A-xy-TPEP) as a new PET radiotracer for noninvasive monitoring of MDR transport function in several xenografted tumor models. It is important to note that MDR is often mediated by a combination of MDR Pgps (particularly MDR1 Pgp) and MRPs. In addition, MDR Pgps and MRPs are also overexpressed in several normal organs involved in excretory functions, including kidneys and liver (58–60).

EXPERIMENTAL SECTION

Materials

Chemicals were purchase from *Sigma*/*Aldrich* (St. Louis, MO). ^{64}Cu was produced using a CS-15 biomedical cyclotron at Washington University School of Medicine by the ^{64}Ni (p,n)^{64}Cu nuclear reaction. $Na^{99m}TcO_4$ was obtained from a commercial DuPont Pharma ^{99}Mo/^{99m}Tc generator. Cardiolite® vials were obtained as a gift from Bristol Myers Squibb Medical Imaging (N. Billerica, MA), and were reconstituted according to the manufacturer's package insert.

Methods

Radio-HPLC method used the LabAlliance HPLC system equipped with a UV/vis detector (λ = 254 nm), a β-ram IN-US detector and Zorbax C_{18} analytical column (4.6 mm × 250 mm, 300 Å pore size). The flow rate was 1 mL/min with the mobile phase being isocratic with 90% solvent A (10 mM ammonium acetate) and 10% solvent B (acetonitrile) at 0 – 5 min, followed by a gradient mobile phase going from 10% B at 5 min to 60% B at 20 min.

Doses Preparation

^{64}Cu(DO3A-xy-TPEP) was prepared according to the procedure described in our previous report (39), and was purified by HPLC. Volatiles in the HPLC mobile phases were evaporated under the reduced pressure at room temperature. Doses were prepared by dissolving the residue to 20 – 30 μCi/mL in saline. The resulting solution was filtered with a 0.20 micron filter unit before being injected into animals. The injection volume for each animal was 0.1 mL.

Animal Models

Biodistribution studies were performed in compliance the NIH animal experiment guidelines (*Principles of Laboratory Animal Care*, NIH Publication No. 86-23, revised 1985). The animal protocol has been approved by the Purdue University Animal Care and Use Committee (PACUC). Female athymic nu/nu mice (5 – 6 weeks) were purchased from Harlan (Charles River, MA). The mice were implanted with 5×10^6 tumor cells into the mammary fat pad (MDA-MB-231 and MDA-MB-435 breast tumor cells) or shoulder flank (U87MG glioma, KB-3-1 and KB-v-1). U87MG glioma cells were cultured in the Minimum Essential Medium, Eagle with Earle's Balanced Salt Solution (non-essential amino acids sodium pyruvate) (ATCC, Manassas, VA). The MDA-MB-435 and MDA-MB-231 breast cancer cells were grown in the RPMI Medium 1640 with L-Glutamine (GIBCO, Grand Island, NY). The DMEM medium with 4.5g/L D-Glucose, L-Glutamine and 110 mg/L sodium pyruvate (GIBCO, Grand Island, NY) was used for KB-v-1 and KB-3-1 tumor cells. In all cases, 10% FBS (Sigma, St.

Louis, MO) and 5% Penicillin Streptomycin (GIBCO, Grand Island, NY) were added into the medium just before use. All cell lines were grown in humidified atmosphere of 5% carbon dioxide. All procedures will be performed in a laminar flow cabinet using the aseptic technique. Two to four weeks after inoculation, the tumor size was in the range of 0.1 – 0.5 g, and animals were used for biodistribution studies.

Biodistribution Protocol

Twelve tumor-bearing mice (20 – 25 g) were divided into four groups. Each animal was administered with ^{64}Cu(DO3A-xy-TPEP) (2 – 3 μCi) via tail vein. Three animals were euthanized by sodium pentobarbital overdose (100 mg/kg) at 5, 30, 60, and 120 min postinjection (p.i.). Blood samples were withdrawn from the heart. The tumor and normal organs (brain, eyes, heart, intestine, kidneys, liver, lungs, muscle and spleen,) were excised, washed with saline, dried with absorbent tissue, weighed, and counted on a Perkin Elmer Wizard – 1480 γ-counter (Shelton, CT). The organ uptake was calculated as a percentage of the injected dose per organ (%ID/organ). The tumor uptake values are reported as an average ± standard deviation based on the results from three tumorbearing mice, unless specified, at each time point. The normal organ uptake values are reported as an average ± standard deviation based on the results from fifteen tumor-bearing mice (3 animals for each tumor type, and a total of five different tumor types) at each time point, unless specified. For comparison purposes, ^{99m}Tc-Sestamibi was evaluated using the same protocol. Comparison between ^{64}Cu (DO3Axy-TPEP) and ^{99m}Tc-Sestamibi was made using the one-way ANOVA test (GraphPad Prim 5.0, San Diego, CA). The level of significance was set at $p < 0.05$.

Blocking Experiment with Cyclosporin-A (Cys-A)

In this experiment, each tumor-bearing mice (n = 4) was treated with intraperitoneal injection of 0.1 mL DMSO solution containing 0.35 mg Cys-A (14 mg/kg) at 30 min before administration of radiotracer. In the “control” group (n = 4), each tumorbearing mouse was treated with the same volume of DMSO solution without Cys-A. Four animals were euthanized by sodium pentobarbital overdose (100 – 200 mg/kg) at 30 min p.i. The ex-vivo biodistribution was performed according to the procedure described above. The organ of uptake was calculated as a percentage of the injected dose per gram (%ID/g).

Subcelluar Distribution Characteristics

Subcellular distribution studies were performed using the athymic nude mice bearing U87MG glioma (n = 3) and MDA-MB-435 breast cancer (n = 3) xenografts according to literature method (61–66). Each tumor-bearing mouse was administered with ~30 μCi of ^{64}Cu(DO3A-xy-TPEP) via tail vein. Animals were sacrificed by intraperitoneal administration of sodium pentobarbital overdose (100 – 200 mg/kg) at 1 h p.i. The tumor was rapidly removed, and placed immediately in ice-cold (4 °C) Buffer I, containing 230 mM mannitol, 70 mM sucrose, 3 mM 3-(N-morpholino)propanesulfonic acid (MOPS), 2 mM ethylene glycol tetraacetic acid (EGTA), and 0.2 % bovine serum albumin (BSA) (w/v) with pH 7.2. The tumor tissue was then minced into 1 – 2 mm pieces, and homogenized using a tissue grinder (Wheaton, NJ). The resulting mixture was centrifuged at 500xg for 10 min at 4 °C. The supernatant (blood, extracellular components and debris) was discarded and pellet was re-suspended in 2 mL of ice-cold (4 °C) Buffer II (containing 110 mM KCl, 20 mM MOPS, 46 mM mannitol, 14 mM sucrose, 2 mM EGTA, pH 7.5). To the mixture was added 0.5 mg/mL of Trypsin protease (Gibco, Ground Island, NY). After 3 min homogenization, the protease reaction was terminated by adding 4 mL of Buffer II (4 °C) containing 0.2 % BSA. The homogenate was centrifuged at 5000xg for 5 min at 4 °C. Supernatant I was collected, and the pellet was re-suspended in 5 mL of ice-cold (4 °C) Buffer II with 0.2% BSA. After centrifugation at 500xg for 10 min (4 °C), pellet I (containing cellular fragments) was obtained. The supernatant was transferred and

centrifuged at 3000xg for 10 min (4 °C) to obtain the membrane fragment (supernatant II) and mitochondrial component (pellet II), respectively. Supernatant I, supernatant II, pellet I and pellet II were counted by a Perkin-Elmer Wizard – 1480 automatic γ-counter (Shelton, CT). The percentage of radioactivity was calculated on the basis of the radioactivity counts in each subcellular component over the total radioactivity count before homogenization. The percentage of radioactivity recovery was calculated by the total radioactivity counts in supernatant I, supernatant II, pellet I and pellet II over the total radioactivity count before homogenization. All data were reported as an average of three independent measurements. ^{99m}Tc-Sestamibi was evaluated using the same protocol for comparison purposes.

Western Blot Experiment

Western blot experiments were performed to demonstrate the presence or absence of MDR1 Pgp, MRP2 and MRP4 in different tumor tissues (U87MG glioma, MDA-MB-231, MDA-MB-435, KB-3-1 and KB-v-1). The tumor tissues (U87MG, MDA-MB-231, MDA-MB-435, KB-3-1 and KB-v-1) were harvested directly from the tumor-bearing nude mice. After homogenized, the tumor tissues (10 – 20 mg) were incubated with 500 μL of cell lysis buffer (Cell Signaling Technology, Danvers, MA) on ice for 5min. The homogenates were centrifuged at 14,000xg for 10 min. The supernatants were removed for further use. For tumor cells, MDA-MB-231 and MDA-MB-435, medium was removed at first. After washed with PBS, cells were incubated with cell lysis buffer (Cell Signaling Technology, Danvers, MA) on ice for 5 min. The tumor cells were scraped and the mixture was sonicated briefly. The homogenates were centrifuged at 14,000xg for 10 min. The supernatant was removed for further use. The protein content was determined by using the BCA™ Protein Assay Kit (Pierce, Rockford, IL). The protein (15 μg per lane) was subjected to electrophoresis on SDS– polyacrylamide gel at 160V for 60 min and transferred electrophoretically on polyvinylidene difluoride membranes at 70 mA for 120 min. The blots were blocked with TBS-T containing 5% non-fat dry milk powder for 1 h. Then, the blotting membranes were incubated with 1 mL of the primary antibody (1:200) against MDR1 (JSB-1, mouse IgG_1 supernatant, Santa Cruz Biotechnology, CA), MRP2 (M2II-12, mouse IgG2a supernatant, Santa Cruz Biotechnology, CA) or MRP4 (M4I-10, rat IgG2a supernatant, Santa Cruz Biotechnology, CA) separately over night. Primary antibody solution was removed and the membranes were incubated for 1 h with secondary antibody (goat anti-mouse IgG-HRP, Santa Cruz Biotechnology, CA) diluted with 1:5000. Finally, membranes were developed using the ECL Western Blotting Substrate (Pierce, Rockford, IL) according to the manufacturer's instructions. The positive control for MDR1 was Human PGP Membrane from BD Gentest (San Jose, CA). Human MRP2 Membrane (BD Gentest, San Jose, CA) was used as the positive control of MRP2.

RESULTS

Biodistribution Characteristics

The athymic nude mice bearing U87MG, MDA-MB-231, MDA-MB-435, KB-3-1 and KB-v-1 tumor xenografts were used to evaluate tumor uptake and biodistribution characteristics of ^{64}Cu(DO3A-xy-TPEP). For comparison purpose, ^{99m}Tc-Sestamibi was also evaluated in the same animal model since it has been clinically used for early cancer detection and for imaging MDR transport function in cancer patients (21–27,30). Biodistribution data for ^{64}Cu (DO3A-xy-TPEP) and ^{99m}Tc-Sestamibi are summarized in Table 1 and Table 2, respectively. Figure 2 compares the tumor uptake (%ID/g) of ^{64}Cu(DO3A-xy-TPEP) and ^{99m}Tc-Sestamibi. Figure 3 illustrates the tumor uptake differences between U87MG glioma and the MDR-positive tumors (MDA-MB-231, MDA-MB-435, KB-3-1 and KB-v-1) for ^{64}Cu(DO3A-xy-TPEP) and ^{99m}Tc-Sestamibi.

In general, the biodistribution of ^{64}Cu(DO3A-xy-TPEP) in non-cancerous organs of the MDRpositive tumor-bearing mice was almost identical to that obtained from the mice bearing U87MG human glioma xenografts. There was no size-dependence for the tumor uptake of ^{64}Cu(DO3A-xy-TPEP) and ^{99m}Tc-Sestamibi. However, ^{64}Cu(DO3A-xy-TPEP) and ^{99m}Tc-Sestamibi showed significant differences in their uptake in both tumors and normal organs. For example, ^{64}Cu(DO3A-xy-TPEP) had a rapid tumor washout in the MDR-negative glioma model between 5 min (5.27 ± 1.21 %ID/g) and 30 min (2.09 ± 0.53 %ID/g) p.i. due to its fast blood clearance, and a steady tumor uptake increase between 30 min (2.09 ± 0.53 %ID/g) and 120 min (3.35 ± 1.27 %ID/g) p.i. probably due to its slow kinetics to penetrate the cellular and mitochondrial transmembranes (39). In the MDR-positive tumor-bearing mice, ^{64}Cu(DO3A-xy-TPEP) showed a rapid tumor washout between 5 and 30 min p.i. (Figure 3: top), and its tumor uptake was relatively unchanged (ranging from 1.0 %ID/g to 1.5 %ID/g depending on the tumor type) in between 30 and 120 min p.i. The tumor uptake of ^{99m}Tc-Sestamibi decreased steadily in all four tumor-bearing animal models over the 2 h period (Figure 3: bottom). The most striking difference between ^{64}Cu(DO3A-xy-TPEP) (Table 1) and ^{99m}Tc-Sestamibi (Table 2) was their uptake in heart and muscle. For example, the heart uptake was <1% ID/g for ^{64}Cu(DO3A-xy-TPEP) at >30 min p.i., whereas ^{99m}Tc-Sestamibi had the heart uptake of 19.22 ± 7.62 % ID/g at 5 min p.i. and 19.19 ± 5.32 %ID/g at 120 min p.i. The muscle uptake of ^{64}Cu(DO3A-xy-TPEP) was undetectable at >30 min p.i. In contrast, ^{99m}Tc-Sestamibi had a high muscle uptake over the 2 h study period (4.84 ± 1.22 and 5.45 ± 1.24 %ID/g at 5 and 120 min p.i., respectively). Another significant difference was their tumor uptake in the MDR-negative U87MG glioma and the MDR-positive tumor xenografts. For example, ^{64}Cu(DO3A-xy-TPEP) had the tumor uptake of 5.27 ± 0.99, 2.09 ± 0.53, 2.58 ± 0.31, and 3.35 ± 1.27 %ID/g at 5, 30, 60 and 120 min p.i., respectively, in U87MG glioma. Its tumor uptake values in the MDR-positive tumors were significantly lower than that in glioma (Figure 2). The glioma uptake values of ^{99m}Tc-Sestamibi were 3.06 ± 0.94, 2.11 ± 0.38, 1.47 ± 0.54, and 1.55 ± 0.36 %ID/g at 5, 30, 60 and 120 min p.i., respectively, and its uptake values in the MDA-MB-435 breast tumor were 1.18 ± 0.17, 1.09 ± 0.20, 0.96 ± 0.42, and 0.94 ± 0.21%ID/g at 5, 30, 60 and 120 min p.i., respectively.

Western Blot Experiments

Western blot experiments were performed to demonstrate the presence or absence of MDR1 Pgp, MRP2 and MRP4 in the U87MG, MDA-MB-231, MDA-MB-435, KB-3-1 and KB-v-1 tumor xenografts. Tumor cells were directly isolated from the tumor tissues. The total protein concentration was determined to be 4.5 ± 0.4, 4.0 ± 0.2, 3.3 ± 0.2, 4.3 ± 0.3 and 4.1 ± 0.2 mg/mL for the xenografted MDA-MB-435, MDA-MB-231, U87MG, KB-v-1 and KB-3-1 tumors, respectively. Figure 4 illustrates the Western blotting data for the U87MG, MDA-MB-231, MDA-MB-435, KB-3-1 and KB-v-1 tumor xenografts. The positive control was the Human PGP Membrane for MDR1 Pgp. The positive control for MPR2 was Human MRP2 Membrane. No positive control is commercially available for MRP4. The blotting data clearly demonstrated that there was very little or no expression of MDR1 Pgp, MRP2 and MRP4 in the U87MG glioma xenografts. However, there is a high expression of MDR1 Pgp, MRP2 and MRP4 in the MDA-MB-231, MDA-MB-435, KB-3-1 and KB-v-1 tumors.

It is important to note that MDA-MB-435 and MDA-MB-231 are often known “drug sensitive” or MDR1-negative breast cancer cell lines (47,48). The results from Western blotting studies also showed that the MDA-MB-435 and MDA-MB-231 human breast cancer cell lines have little expression of MDR1 Pgp (Figure 4B). However, the MDA-MB-435 and MDA-MB-231 breast cancer cells isolated from the xenografted MDA-MB-435 and MDA-MB-231 breast tumors are MDR1-positive (Figure 4B). They also show a significant expression of MRP2 and MRP4.

Impact of Cys-A on Tumor Uptake and Radiotracer Liver Clearance Kinetics

To further demonstrate that the tumor washout is caused by the tumor MDR transport function, we performed blocking experiments using ^{64}Cu(DO3A-xy-TPEP) and ^{99m}Tc-Sestamibi as radiotracers in the athymic nude mice bearing KB-3-1 and KB-v-1 tumor xenografts. Cys-A, a well-known wide-spectrum MDR modulator (67), was injected as the blocking agent 1 h prior administration of ^{64}Cu(DO3A-xy-TPEP) or ^{99m}Tc-Sestamibi. The ex-vivo biodistribution was performed at 30 min p.i. Figure 5 compares uptake of ^{64}Cu(DO3A-xy-TPEP) and ^{99m}Tc-Sestamibi in the tumor and selected normal organs in the absence/presence of Cys-A. As expected, pre-treatment of the tumor-bearing mice with excess Cys-A resulted in a significant increase in tumor uptake of both ^{64}Cu(DO3A-xy-TPEP) (Figure 5: bottom) and ^{99m}Tc-Sestamibi (Figure 5: top). The tumor uptake difference was 0.83 %ID/g in KB-3-1 and 1.70 KBv-1 %ID/g w/o Cys-A for ^{64}Cu(DO3A-xy-TPEP) while there was no significant difference for ^{99m}Tc-Sestamibi within the experimental error, suggesting that ^{64}Cu(DO3A-xy-TPEP) might be a more efficient radiotracer for noninvasive monitoring of the MDR transport function.

In addition, the uptake of ^{64}Cu(DO3A-xy-TPEP) and ^{99m}Tc-Sestamibi in kidneys, liver and lungs, was also significantly increased, and the radioactivity excretion was delayed in the presence of Cys-A. For example, the liver uptake was 8.03 ± 1.33 %ID/g for ^{64}Cu(DO3A-xy-TPEP) and 9.82 ± 2.12 %ID/g for ^{99m}Tc-Sestamibi in the absence of Cys-A at 30 min p.i. In presence of Cys-A, however, the liver uptake values increased to 17.18 ± 2.47 %ID/g for ^{64}Cu(DO3A-xy-TPEP) and 23.68 ± 5.08 %ID/g for ^{99m}Tc-Sestamibi at the same time point. Similar increase (Figure 5) was also observed in the heart, kidneys, lungs and spleen. The increase of muscle uptake of ^{64}Cu(DO3A-xy-TPEP) is probably caused by its high blood radioactivity accumulation in the presence of excess Cys-A. The impact of Cys-A on the excretion kinetics of ^{64}Cu(DO3A-xy-TPEP) was more significant than that of ^{99m}Tc-Sestamibi.

Subcellular Distribution Characteristics

We performed the subcellular distribution studies on ^{64}Cu(DO3A-xy-TPEP) and ^{99m}Tc-Sestamibi using the standard differential centrifugation method (Figure 6) according to the literature (61–65). The main objective of these studies is to elucidate the tumor localization mechanism of ^{64}Cu(DO3A-xy-TPEP). Figure 7 illustrates the subcellular distribution characteristics of ^{64}Cu(DO3A-xy-TPEP) and ^{99m}Tc-Sestamibi in the xenografted U87MG glioma and MDA-MB-435 tumors. The radioactivity recovery was >95% for both ^{64}Cu (DO3A-xy-TPEP) and ^{99m}Tc-Sestamibi. After cellular fractionation, majority of the radioactivity was found in supernatants I (66.5 ± 12.5% for ^{64}Cu(DO3A-xy-TPEP) and 63.5 ± 4.7% for ^{99m}Tc-Sestamibi) and II (8.5 ± 0.5% for ^{64}Cu(DO3A-xy-TPEP) and 14.5 ± 2.6% for ^{99m}Tc-Sestamibi). Only a small portion of the radioactivity was found in the mitochondrial fraction (Figure 7: top) for ^{64}Cu(DO3A-xy-TPEP) (2.25 ± 0.21%) and ^{99m}Tc-Sestamibi (3.33 ± 1.50%). It is clear that ^{64}Cu(DO3A-xy-TPEP) and ^{99m}Tc-Sestamibi share almost identical subcellular distribution patterns in the U87MG glioma tumors. In addition, the subcellular distribution characteristics of ^{64}Cu(DO3A-xy-TPEP) are very similar in the xenografted U87MG glioma and MDA-MB-435 breast tumors (Figure 6: bottom).

DISCUSSION

During last two decades, cationic radiotracers, such as ^{99m}Tc-Sestamibi, have been widely used for early cancer detection and for noninvasive monitoring of the tumor MDR transport function by SPECT (21–35). The overwhelming emphasis of the prior literature has been focused on the tumor MDR transport function mediated by MDR1 Pgp most likely due to the fact that MDR1 Pgp is one of the best biologically characterized barriers to chemotherapy. It

is very important to emphasize that the tumor MDR transport function can be mediated by MDR Pgps and MRPs (1–11), as well as other drug transporting proteins, such as LRP (17) and BCRP (18). Regardless of the source of MDR, the overall net effect is the rapid efflux of cationic radiotracers from tumor cells, which often leads to a significant reduction of the radiotracer tumor uptake. There is an inverse relationship between the radiotracer tumor uptake and the MDR transport function. If there is no MDR Pgps and/or MRPs in tumor cells, cationic radiotracers will have relatively high tumor uptake with no significant tumor washout. If there is a high level expression of MDR Pgps and/or MRPs, cationic radiotracers are expected to show a rapid tumor radioactivity washout with low tumor uptake. If the radiotracer is efficient as a substrate for MDR Pgps and MRPs, there would be less radiotracer uptake in the MDR-positive tumors. The ideal radiotracers useful for noninvasive monitoring of the tumor MDR transport function would be those which provide the largest uptake difference between the MDR-negative and MDR-positive tumors, and have low uptake in non-cancerous organs, such as the heart, liver, lungs and muscle.

Since the uptake of ^{64}Cu(DO3A-xy-TPEP) in normal organs is almost identical in different xenografted tumor-bearing models, their tumor uptake difference should, in theory, reflect the MDR transport function in the MDR-negative vs. MDR-positive tumors. For example, the U87MG glioma tumors have no significant expression of MDR1 Pgp and MRPs, as demonstrated by Western blot experiment (Figure 4). As a result, ^{64}Cu(DO3A-xy-TPEP) has a high initial tumor uptake, and show a steady uptake increase between 30 and 120 min p.i. (Figure 2: top). Similar results are obtained for ^{99m}Tc-Sestamibi (Figure 2: bottom). The xenografted MDA-MB-435, MDA-MB-231, KB-3-1 and KBv-1 tumors all have high levels of MDR1 Pgp, MRP2 and MRP4 expression (Figure 4A). As a result, both ^{64}Cu(DO3A-xy-TPEP) and ^{99m}Tc-Sestamibi show a significant washout from tumor over the 2 h period. Since ^{64}Cu(DO3A-xy-TPEP) has a greater tumor uptake difference between U87MG glioma and MDA-MB-231, MDA-MB-435, KB-3-1 and KB-v-1 than ^{99m}Tc-Sestamibi, it is reasonable to believe that ^{64}Cu(DO3A-xy-TPEP) is more efficient than ^{99m}Tc-Sestamibi as the substrate for MDR Pgps and MRPs, and might be more efficient for noninvasive monitoring of the tumor MDR transport function. This conclusion is supported by the blocking experiments, which show a significant tumor uptake increase for ^{64}Cu(DO3A-xy-TPEP) and ^{99m}Tc-Sestamibi in the presence of excess Cys-A (Figure 5).

Both ^{99m}Tc-Sestamibi and ^{99m}Tc-Tetrafosmin have been studied for their potential to monitor the tumor MDR in pre-clinical animal models and in clinical studies (28–35). The MDR1 Pgp and MRPs are also overexpressed in normal organs, such as kidneys and liver (58–60). As demonstrated in the blocking study (Figure 5), the pre-administration of tumor bearing mice with excess Cys-A resulted in a significant increase of radioactivity accumulation in non-cancerous organs, such as kidneys, liver and lungs, and the delayed radioactivity excretion. Therefore, the MDR Pgp transport function is at least partially responsible of the fast efflux of ^{64}Cu(DO3A-xy-TPEP) from the kidneys, liver, and lungs.

The subcellular distribution characteristics of ^{64}Cu(DO3A-xy-TPEP) was compared with those of ^{99m}Tc-Sestamibi, a well-know radiotracer clinically useful for cancer detection by SPECT. The standard differential centrifugation technique has been successfully used to study the myocardial localization mechanism of cationic ^{99m}Tc radiotracers (61–66), such as ^{99m}Tc-Sestamibi. As expected, only a small fraction (3 – 4%) of ^{64}Cu radioactivity is found in the mitochondrial fraction, and majority of the ^{64}Cu radioactivity is found in supernatants I and II. Almost identical distribution patterns were observed for ^{99m}Tc-Sestamibi. It has been suggested the tissue homogenization and differential centrifugation techniques may damage the mitochondrial structure (61–66), which allows the leakage of cationic radiotracers, such as ^{64}Cu(DO3A-xy-TPEP) and ^{99m}Tc-Sestamibi, from tumor mitochondria. Since ^{64}Cu (DO3A-xy-TPEP) and ^{99m}Tc-Sestamibi share almost identical subcellular distribution patterns

in the U87MG glioma, we believe that ^{64}Cu(DO3A-xy-TPEP), like ^{99m}Tc-Sestamibi, is able to localize in the tumor mitochondria due to the increased plasma and mitochondrial transmembrane potentials in tumor cells as compared to normal epithelial cells (68–72). This conclusion is supported by the results from *in vitro* cellular assays, which showed that ^{64}Cu (DO3A-xy-TPP) (DO3A-xy-TPP: triphenyl(4-((4,7,10-tris(carboxymethyl)-1,4,7,10-tetraazacyclododecan-1-yl)methyl)benzyl)phosphonium) was able to localize in U87MG human glioma cells (36).

CONCLUSION

In this study, we evaluated the potential of ^{64}Cu(DO3A-xy-TPEP) as a new PET radiotracer for noninvasive monitoring of MDR transport function in several xenografted tumor models. It is important to note that MDR is often mediated by a combination of MDR Pgps (particularly MDR1 Pgp) and MRPs. ^{64}Cu(DO3A-xy-TPEP) has a high initial tumor uptake and show a steady uptake increase between 30 and 120 min p.i. in the MDR-negative U87MG glioma, which has little expression of MDR1 Pgp and MRPs. In the xenografted MDA-MB-435, MDA-MB-231, KB-3-1 and KB-v-1 tumors, which have high levels of MDR1 Pgp, MRP2 and MRP4, ^{64}Cu(DO3A-xy-TPEP) and ^{99m}Tc-Sestamibi show a significant tumor washout over the 2 h period. Since ^{64}Cu(DO3A-xy-TPEP) has a greater tumor uptake difference between the MDR-negative U87MG glioma and MDR-positive tumors (MDA-MB-231, MDA-MB-435, KB-3-1 and KB-v-1) than ^{99m}Tc-Sestamibi, we believe that ^{64}Cu(DO3A-xy-TPEP) is more efficient than ^{99m}Tc-Sestamibi as the substrate for MDR Pgps and MRPs, and might be a more efficient radiotracer for noninvasive monitoring of the MDR transport function in tumors of different origin. Regardless of the source of MDR, the overall net effect is the rapid efflux of cationic radiotracers from tumor cells, which often leads to a significant reduction of the radiotracer tumor uptake.

Acknowledgment

Authors would like to thank Dr. Sulma I. Muhammed, the Director of Purdue Cancer Center Drug Discovery Shared Resource, Purdue University, for her assistance with the tumor-bearing animal model. This work is supported, in part, by research grants: R01 CA115883 A2 (S.L.) from National Cancer Institute (NCI), R21 EB003419–02 (S.L.) from National Institute of Biomedical Imaging and Bioengineering (NIBIB) and R21 HL083961–01 from National Heart, Lung, and Blood Institute (NHLBI).

REFERENCES

1. Ling V. Multidrug resistance: molecular mechanisms and clinical relevance. Cancer Chemother. Pharmacol 1997;40:S3–S8. [PubMed: 9272126]
2. Gros P, Benneriah YB, Croop JM, Housman DE. Isolation and expression of a complementary DNA that confers multidrug resistance. Nature 1986;323:728–731. [PubMed: 3022150]
3. Zaman GJR, Flens MJ, Vanleusden MR, Dehaas M, Mulder HS, Lankelma J, Pinedo HM, Scheper RJ, Baas F, Broxterman HJ, Borst P. The human multidrug resistance-associated-protein MRP is a plasma-membrane drug-efflux pump. PNAS 1994;91:8822–8826. [PubMed: 7916458]
4. Klein I, Sarkadi B, Varadi A. An inventory of the human ABC proteins. Biochim. Biophys. Acta 1999;1461:237–262. [PubMed: 10581359]
5. Shapiro AB, Ling V. Reconstitution of drug transport by purified P-glycoprotein. J. Biol. Chem 1995;270:16167–16175. [PubMed: 7608182]
6. Mao Q, Deeley RG, Cole SP. Functional reconstitution of substrate transport by purified multidrug resistance protein MRP1 (ABCC1) in phospholipid vesicles. J. Biol. Chem 2000;275:34166–34172. [PubMed: 10942765]
7. Ferté J. Analysis of the tangled relationships between P-glycoprotein-mediated multidrug resistance and the lipid phase of the cell membrane. Eur. J. Biochem 2000;267:277–294. [PubMed: 10632698]

8. Thomas GA, Barrand MA, Stewart S, Rabbitts PH, Williams ED, Tweentyman PR. Expression of the multidrug resistance-associated protein (MRP) gene in human lung tumors and normal tissue as determined by in situ hybridization. Eur. J. Cancer 1994;30:1705–1709. [PubMed: 7833148]
9. Charpin C, Vielh P, Duffaud F, Devictor B, Andrac L, Lavaut MN, Allasia C, Horschowski N, Piana L. Quantitative immunocytochemical assays of Pglycoprotein in breast carcinoma-correlation to messenger-RNA expression and to immunohistochemical prognostic indicators. J. Natl. Cancer Inst 1994;86:1539–1545. [PubMed: 7932810]
10. Hijazi YM, Axiotis CA, Navarro S, Steinberg SM, Horowitz ME, Tsokos M. Immunohistochemical detection of P-glycoprotein in Ewing's sarcoma and peripheral primitive neuroectodermal tumors before and after chemotherapy. Am. J. Clin. Pathol 1994;102:61–67. [PubMed: 7913576]
11. Chan H, Grogan T, Haddad G, DeBoer G, Ling V. P-glycoprotein expression: critical determent in the response to osteosarcoma chemotherapy. J. Natl. Cancer Inst 1997;89:1706–1715. [PubMed: 9390540]
12. Lee JS, Scala S, Matsumoto Y, Dickstein B, Robey R, Zhan Z, Altenberg G, Bates SE. Reduced drug accumulation and multidrug resistance in human breast cancer cells without associated P-glycoprotein or MRP overexpression. J. Cell Biol 1997;65:513–526.
13. Linn SC, van Kalken CK, van Tellingen O, van der Valk P, van Groeningen CJ, Kuiper CM, Pinedo HM, Giaccone G. Clinical and pharmacologic study of multidrug resistance reversal with vinblastine and bepridil. J. Clin. Oncol 1994;12:812–819. [PubMed: 7908691]
14. Lonn U, Lonn S, Nilsson B, Stenkvist B. Intratumoral heterogeneity for amplified genes in human breast carcinoma. Int. J. Cancer 1994;58:40–45. [PubMed: 7912234]
15. Sogier MA, Zhang Y, Eberle RL, Sweet KM, Altenberg GA, Belli JA. Sequestration of doxorubicin in vesciles in a multidrug-resistant cell line (LZ-100). Biochem. Pharmacol 1994;48:391–401. [PubMed: 7914406]
16. Chan H, Lu Y, Grogan T, Haddad G, Hipfner D, Cole S, Deeley R, Ling V, Gallie B. Multidrug resistance protein (MRP) expression in retinoblastoma correlates with the rare failure of chemotherapy despite cyclosporine for reversal of P-glycoprotein. Cancer Res 1997;57:2325–2330. [PubMed: 9192801]
17. Scheffer GL, Wijngaard PL, Flens MJ, Izquierdo MA, Slovak ML, Pinedo HM, Meijor CJ, Clevers HC, Scheper AJ. The drug resistance-related protein LRP is the human major vault protein. Nat. Med 1995;1:578–582. [PubMed: 7585126]
18. Litman T, Brangi M, Hudson E, Fetsch P, Abati A, Ross DD, Miyake K, Resau JH, Bates SE. The multidrug-resistant phenotype associated with overexpression of the new ABC half-transporter, MXR (ABCG2). J. Cell Sci 2000;113:2011–2021. [PubMed: 10806112]
19. Wang Y, Pan XQ, L'Heureux F, Georges E. Overexpression of 40-kDa protein in human multidrug resistant cells. Biochem. Biophys. Res. Commun 1997;236:483–488. [PubMed: 9240465]
20. Wang Y, Serfass L, Roy MO, Wong J, Bonneau AM, Georges E. Annexi-I expression modulate drug resistance in tumors cells. Biochem. Biophys. Res. Commun 2004;314:565–570. [PubMed: 14733945]
21. Del Vecchio S, Salvatore MR. ^{99m}Tc-MIBI in the evaluation of breast cancer biology. Eur. J. Nucl. Med. Mol. Imaging 2004;31:S88–S96. [PubMed: 15105972]
22. Schomäcker K, Schicha H. Use of myocardial imaging agents for tumor diagnosisa success story? Eur. J. Nucl. Med 2000;27:1845–1863. [PubMed: 11189949]
23. Sharma V. Radiopharmaceuticals for assessment of multidrug resistance P-glycoprotein-mediated drug transport activity. Bioconj. Chem 2004;15:1464–1474.
24. Sharma V, Piwnica-Worms D. Monitoring multidrug resistance P-glycoprotein drug transport activity with single-photon emission computed tomography and positron emission tomography radiopharmaceuticals. Topics Curr. Chem 2005;252:155–178.(Contrast Agents III)
25. Vaidyanathan G, Zalutsky MR. Imaging drug resistance with radiolabeled molecules. Current Pharm. Design 2004;10:2965–2979.
26. Mazzammil T, Ballinger JR, Moore MJ. ^{99}Tc^{m}-sestamibi imaging of inhibition of the multidrug resistance transporter in a mouse xenograft model of human breast cancer. Nucl. Med. Commun 1999;20:115–122. [PubMed: 10088159]

27. Filippi L, Santoni R, Manni C, Danieli R, Floris R, Schillaci O. Imaging primary brain tumor by single-photon emission computed tomography (SPECT) with technetium-99m Sestamibi (MIBI) and Tetrofosmin. Current Med. Imag. Rev 2005;1:61–66.
28. Herman LW, Sharma V, Kronauge JF, Barbarics E, Herman LA, Piwnica-Worms D. Novel hexakis (areneisonitrile)technetium(I) complexes as radioligands targeted to the multidrug resistance P-glycoprotein. J. Med. Chem 1995;38:2955–2963. [PubMed: 7636856]
29. Muzzammil T, Ballinger JR, Moore MJ. ^{99m}Tc-sestamibi imaging of inhibition of the multidrug resistance transporter in a mouse xenograft model of human breast cancer. Nucl. Med. Commun 1999;20:115–122. [PubMed: 10088159]
30. Agrawal M, Abraham J, Balis FM, Edgerly M, Stein WD, Bates S, Fojo T, Chen CC. Increased ^{99m}Tc-Sestamibi accumulation in normal liver and drug resistant-tumors after the administration of the glycoprotein inhibitor, XR9576. Clin. Cancer Res 2003;9:650–656. [PubMed: 12576431]
31. Liu ZL, Stevenson GD, Barrett HH, Kastis GA, Bettan M, Furenlid LR, Wilson DW, Woolfenden JM. Imaging recognition of drug resistance in human breast tumors using ^{99m}Tc-labeled monocationic agents and a high-resolution stationary SPECT system. Nucl. Med. Biol 2004;31:53–65. [PubMed: 14741570]
32. Liu ZL, Stevenson GD, Barrett HH, Furenlid LR, Wilson DW, Kastis GA, Bettan M, Woolfenden JM. Imaging recognition of inhibition of drug resistance in human breast cancer xenografts using ^{99m}Tc-labeled sestamibi and tetrofosmin. Nucl. Med. Biol 2005;32:573–583. [PubMed: 16026704]
33. Luker GD, Francisco PM, Dobkin J, Piwbica-Worms D. Modulation of the multidrug resistance P-glycoprotein: Detection with technetium-99m sestamibi in vivo. J. Nucl. Med 1997;38:369–372. [PubMed: 9074520]
34. Márián T, Szabó G, Nagy H, Szincsák N, Juhász I, Galuska L, Balkay L, Mikecz P, Trón L, Krasznai Z. In vivo and in vitro multitracer analysis of P-glycoprotein expression-related multidrug resistance. Eur. J. Nucl. Med. Mol. Imaging 2003;30:1147–1154. [PubMed: 12830325]
35. Lorker DE, Krüger M, Buchert R, Bohuslavizki KH, Clausen M, Schumacker U. In vitro and in vivo tracer characteristics of an established multidrug-resistant human colon cancer cell line. J. Nucl. Med 2001;42:646–654. [PubMed: 11337555]
36. Wang J, Yang CT, Kim YS, Sreerama SG, Cao Q, Li Z, He Z, Chen X, Liu S. ^{64}Cu-Labeled triphenylphosphonium and triphenylarsonium cations as highly tumor-selective PET imaging agents. J. Med. Chem 2007;50:5057–5069. [PubMed: 17867662]
37. Kim YS, Yang CT, Wang JJ, Sreerama SG, Cao Q, Li Z, He Z, Chen X, Liu S. Radiolabeled triphenylphosphonium cations as highly tumor-selective imaging agents: Effects of radiometals, bifunctional chelators and molecular charge. J. Med. Chem 2008;51:2971–2984. [PubMed: 18419113]
38. Yang CT, Li YX, Liu S. Synthesis and structural characterization of complexes of a DO3A-conjugated triphenylphosphonium cation with diagnostically important metal ions. Inorg. Chem 2007;46:8988–8997. [PubMed: 17784751]
39. Yang CT, Kim YS, Wang J, Wang L, Shi J, Li Z, Chen X, Fan M, Li JJ, Liu S. ^{64}Cu-labeled 2-(Diphenylphosphoryl)ethyldiphenylphosphonium cations as highly selective tumor imaging agents: effects of linkers and chelates on biodistribution characteristics. Bioconj. Chem 2008;19:2008–2022.
40. Bähr O, Wick W, Weller M. Modulation of MDR/MRP by wild-type and mutant p53. J. Clin. Invest 2001;107:643–645. [PubMed: 11238567]
41. Bähr O, Rieger J, Duffner F, Meyermann R, Wller M, Wick W. P-glycoprotein and multidrug resistance-associated protein mediate specific patterns of multidrug resistance in malignant glioma cell lines, but not in primary glioma cells. Brain Pathol 2003;13:482–494. [PubMed: 14655754]
42. Nakatsu S, Kondo S, Kondo Y, Yin D, Peterson JW, Kaakaji R, Morinura T, Kikuchi H, Takeuchi J. Induction of apoptosis in multi-drug resistant (MDR) human glioblastoma cells by SN38, a metabolite of the camptothecin derivative CPT-11. Cancer Chemother. Pharmacol 1977;39:417–423. [PubMed: 9054955]
43. Le Jeune N, Perek N, Denover D, Dubois F. Influence of gluthione depletion on plasma membrane cholesterol esterification and on Tc-99m-Sestamibi and Tc-99m-Tetrofosmin uptakes; a comparative study in sensitive U87MG and multidrug-resistant MRP1 human glioma cells. Cancer Biother. Radiopharm 2004;19:411–421. [PubMed: 15453956]

44. Ihnat MA, Lariviere JP, Warren AJ, Ronde NL, Blaxall JRN, Pierre KM, Turpie BW, Hamilton JW. Suppression of P-glycoprotein expression and multidrug resistance by DNA cross-linking agents. Clin. Cancer Res 1997;3:1339–1346. [PubMed: 9815817]
45. Matsumoto Y, Takano H, Kunishio K, Nagao S, Fojo T. Expression of drug resistance genes in VP-16 and mAMSA-selected human carcinoma cells. Jpn. J. Cancer Res 2001;92:778–784. [PubMed: 11473729]
46. Liu BL, Sun DT, Xia WY, Hung MC, Yu DH. Cross-reactivity of C219 anti-$p170^{mdr-1}$ antibody with $p185^{c-erbB2}$ in breast cancer cells: cautions on evaluating $p170^{mdr-1}$. Journal of National Cancer Institute 1997;89:1524–1529.
47. Engel JB, Schally AV, Halmos G, Baker B, Nagy A, Keller G. Targeted cytotoxicity bombesin analog AN-215 effectively inhibits experimental human breast cancer with low induction of multi-drug resistance proteins. Endocrine-Related Cancer 2005;12:999–1009. [PubMed: 16322338]
48. Savas B, Kerr PE. Lymphokine-activated killer cell susceptibility and adhesion molecule expression of multidrug resistant breast carcinoma. Cancer Cell Int. 2006http://www.cancerci.com/content/6/1/24
49. Sharma V, Prior JL, Belinsky MG, Kruh GD, Piwnica-Worms D. Characterization of a $^{67}Ga/^{68}Ga$ radiopharmaceutical for SPECT and PET of MDR1 P-glycoprotein transport activity in vivo: validation in multidrug-resistant tumors and at the bloodbrain barrier. J. Nucl. Med 2005;46:354–364. [PubMed: 15695797]
50. Ocheskey JA, Polyakov VR, Harpstrite SE, Oksman A, Goldberg DE, Piwnica-Worms D, Sharma V. Synthesis, characterization, and molecular structure of a gallium(III) complex of an amine-phenol ligand with activity against chloroquine-sensitive Plasmodium falciparum strains. J. Inorg. Biochem 2003;93:265–270. [PubMed: 12576290]
51. Dyszlewski M, Blake HM, Dahlheimer JL, Pica CM, Piwnica-Worms D. Characterization of a novel ^{99m}Tc-carbonyl complex as a functional probe of MDR1 Pglycoprotein transport activity. Mol. Imag 2002;1:24–35.
52. Luker GD, Flagg TP, Sha Q, Luker KE, Pica CM, Nichols CG, Piwnica-Worms D. MDR1 P-glycoprotein reduces influx of substrates without affecting membrane potential. J. Biol. Chem 2001;276:49053–49060. [PubMed: 11598111]
53. Slapak CA, Dahlheimer J, Piwnica-Worms D. Reversal of multidrug resistance with LY335979. J. Clin. Pharmacol 2001;41:29S–38S. [PubMed: 11452726]
54. Rao VV, Herman LW, Kronauge JF, Piwnica-Worms D. A novel areneisonitrile Tc complex inhibits the transport activity of MDR P-glycoprotein. Nucl. Med. Biol 1998;25:225–232. [PubMed: 9620627]
55. Crankshaw CL, Marmion M, Luker GD, Rao V, Dahlheimer J, Burleigh BD, Webb E, Deutsch KF, Piwnica-Worms D. Novel technetium (III)-Q complexes for functional imaging of multidrug resistance (MDR1) P-glycoprotein. J. Nucl. Med 1998;39:77–86. [PubMed: 9443741]
56. Luker GD, Rao VV, Crankshaw CL, Dahlheimer J, Piwnica-Worms D. Characterization of phosphine complexes of technetium(III) as transport substrates of the multidrug resistance P-glycoprotein and functional markers of P-glycoprotein at the blood-brain barrier. Biochem 1997;36:14218–14227. [PubMed: 9369495]
57. Pichler A, Prior JL, Piwnica-Worms D. Imaging reversal of multidrug resistance in living mice with bioluminescence: MDR1 P-glycoprotein transports coelenterazine. PNAS. USA 2004;101:1702–1707. [PubMed: 14755051]
58. Gatmaitan ZC, Arias IM. Structure and function of P-glycoprotein in normal liver and small intestine. Adv. Pharmacol 1993;24:77–97. [PubMed: 8099292]
59. Lee CH, Bradley G, Zhang JT, Ling V. Differential expression of Pglycoprotein genes in primary rat hepatocytes culture. J. Cell Physiol 1993;157:392–402. [PubMed: 7901227]
60. Mayer R, Kartenbeck J, Buchler M, Jedlitschky G, Leier I, Keppler D. Expression of the MRP gene-encoded conjugate export pump in liver and its selective absence from the canalicular membrane in transport deficient mutant hepatocytes. J. Cell Biol 1995;131:137–150. [PubMed: 7559771]
61. Carvalho PA, Chiu ML, Kronauge JF, Kawamura M, Jones AG, Holman BL, Piwnica-Worms D. Subcellular distribution and analysis of technetium-99m-MIBI in isolated perfused rat hearts. J. Nucl. Med 1992;33:1516–1521. [PubMed: 1634944]

62. Bolzati1 C, Cavazza-Ceccato M, Agostini S, Tokunaga S, Casara D, Bandoli G. Subcellular distribution and metabolism studies of the potential myocardial imaging agent [^{99m}Tc(N)(DBODC)(PNP5)]$^{+}$ J. Nucl. Med 2008;49:1336–1344. [PubMed: 18632814]
63. Kim YS, Shi J, Hou GH, Liu S. Mechanism for myocardial localization and rapid liver clearance of ^{99m}TcN-MPO: a new heart imaging agent. J. Nucl. Cardiol. Submitted
64. Ochoa S. Malic dehydrogenase from pig heart. Methods Enzymol 1955;1:735–739.
65. Platts EA, North TL, Pickett RD, Kelly JD. Mechanism of uptake of technetium-tetrofosmin I: uptake into isolated adult rat ventricular myocytes and subcellular localization. J. Nucl. Cardiol 1995;2:317–326. [PubMed: 9420806]
66. Younes A, Songadele JA, Maublant J, Platts E, Pickett R, Veyre A. Mechanism of uptake of technetium-tetrofosmin II: uptake into isolated adult rat heart mitochondria. J. Nucl. Cardiol 1995;2:327–333. [PubMed: 9420807]
67. Qadir M, O'Loughlin KL, Fricke SM, Williamson NA, Greco WR, Minderman H, Baer M. Cyclosporin A is a broad-spectrum multidrug resistance modulator. Clin Cancer Res 2005;11:2320–2326. [PubMed: 15788683]
68. Kroemer G, Dallaporta B, Resche-Rigon M. The mitochondrial death/life regulator in apoptosis and necrosis. Annu. Rev. Physiol 1998;60:619–642. [PubMed: 9558479]
69. Modica-Napolitano JS, Aprille JR. Delocalized lipophilic cations selectively target the mitochondria of carcinoma cells. Advanced Drug Delivery Reviews 2001;49:63–70. [PubMed: 11377803]
70. Duchen MR. Mitochondria in health and disease: perspectives on a new mitochondrial biology. Molecular Aspects of Medicine 2004;25:365–451. [PubMed: 15302203]
71. Gottlieb E, Thompson CB. Targeting the mitochondria to enhance tumor suppression. Methods Mol. Biol 2002;223:543–554. [PubMed: 12777750]
72. Mannella CA. The relevance of mitochondrial membrane topology to mitochondrial function. Biochem. Biophys. Acta 2006;1762:140–147. [PubMed: 16054341]

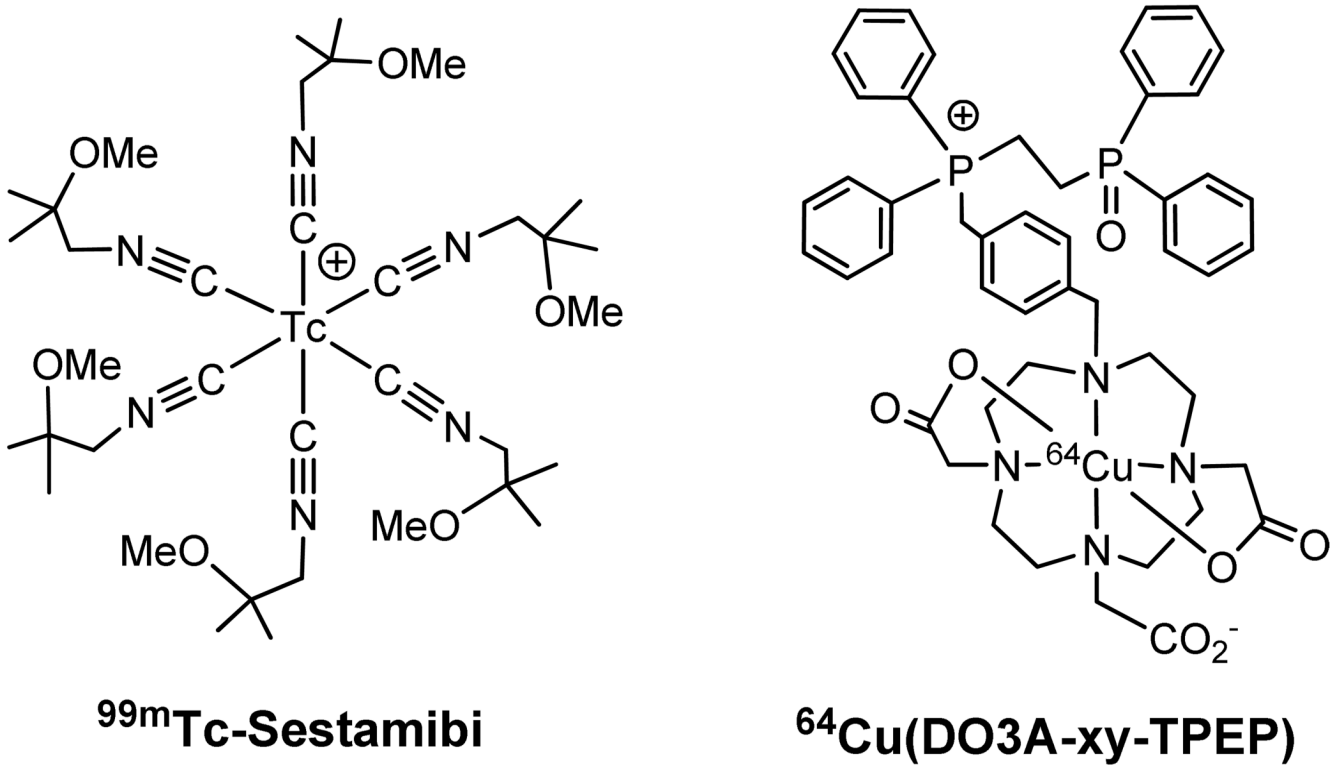

Figure 1.
Structures of ^{99m}Tc-Sestamibi and ^{64}Cu(DO3A-xy-TPP).

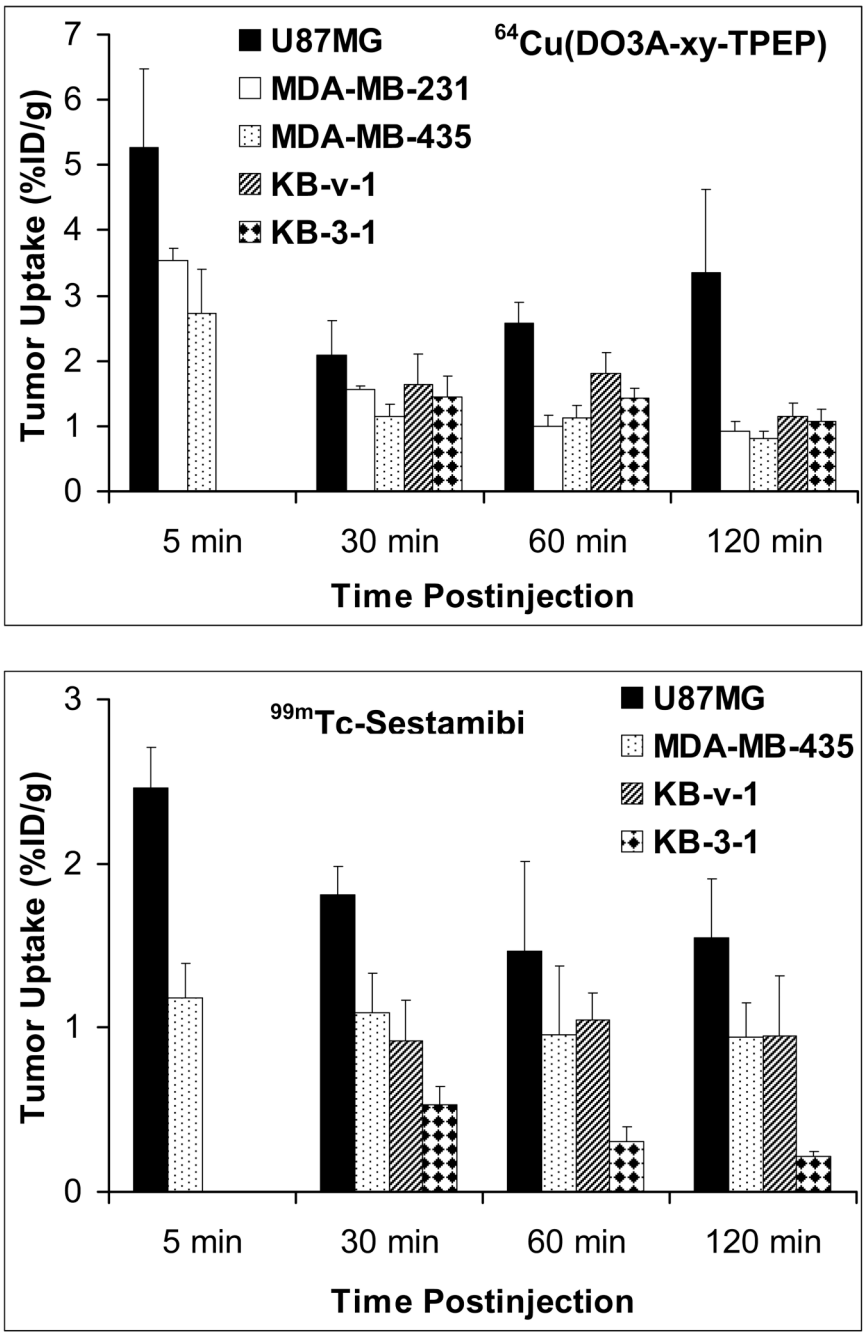

Figure 2.
Comparison of tumor uptake for ^{64}Cu(DO3A-xy-TPEP) (top) and ^{99m}Tc-Sestamibi (bottom) in athymic nude mice bearing different tumor xenografts (U87MG glioma, MDA-MB-231 and MDA-MB-435 breast cancer, KB-3-1 and KB-v-1).

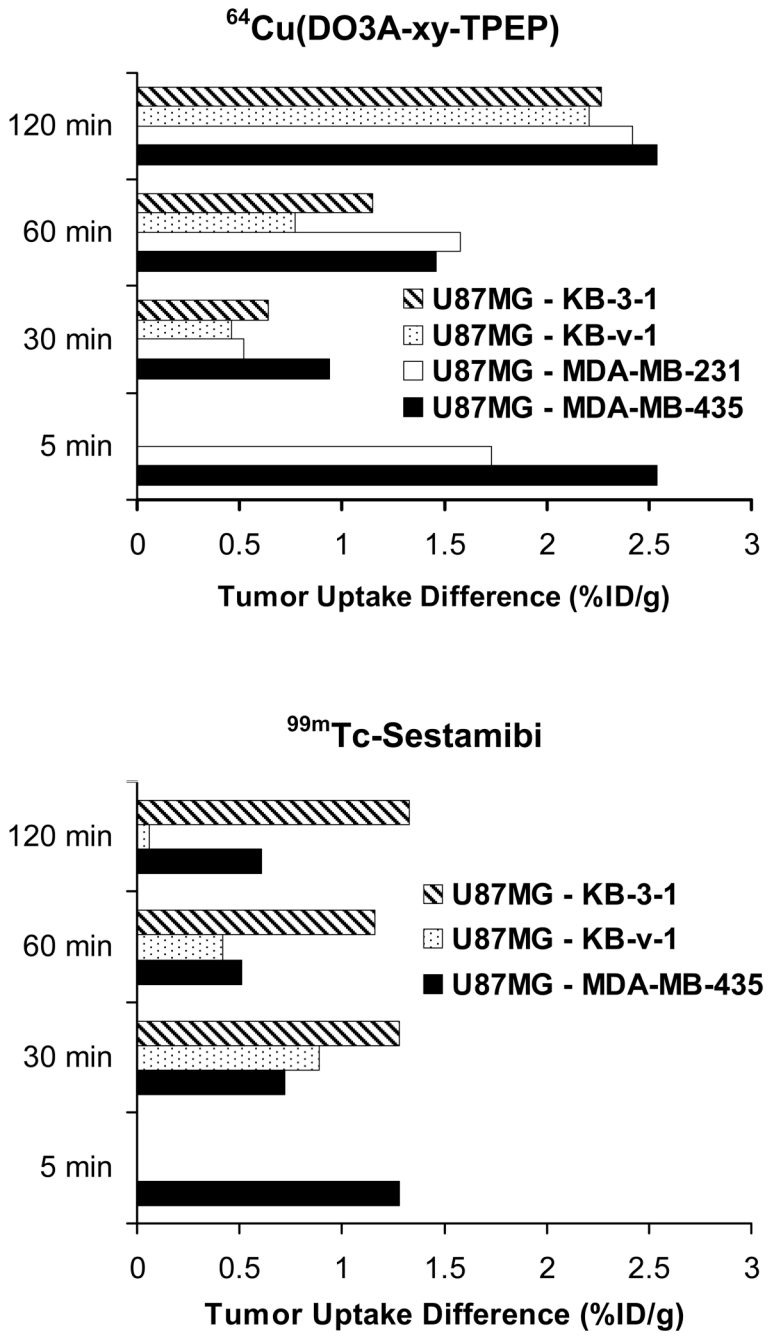

Figure 3.
Tumor uptake difference between the MDR-negative U87MG glioma and the MDR-positive tumors (MDA-MB-231, MDA-MB-435, KB-3-1 and KB-v-1) for ^{64}Cu(DO3A-xy-TPEP) (top) and ^{99m}Tc-Sestamibi (bottom).

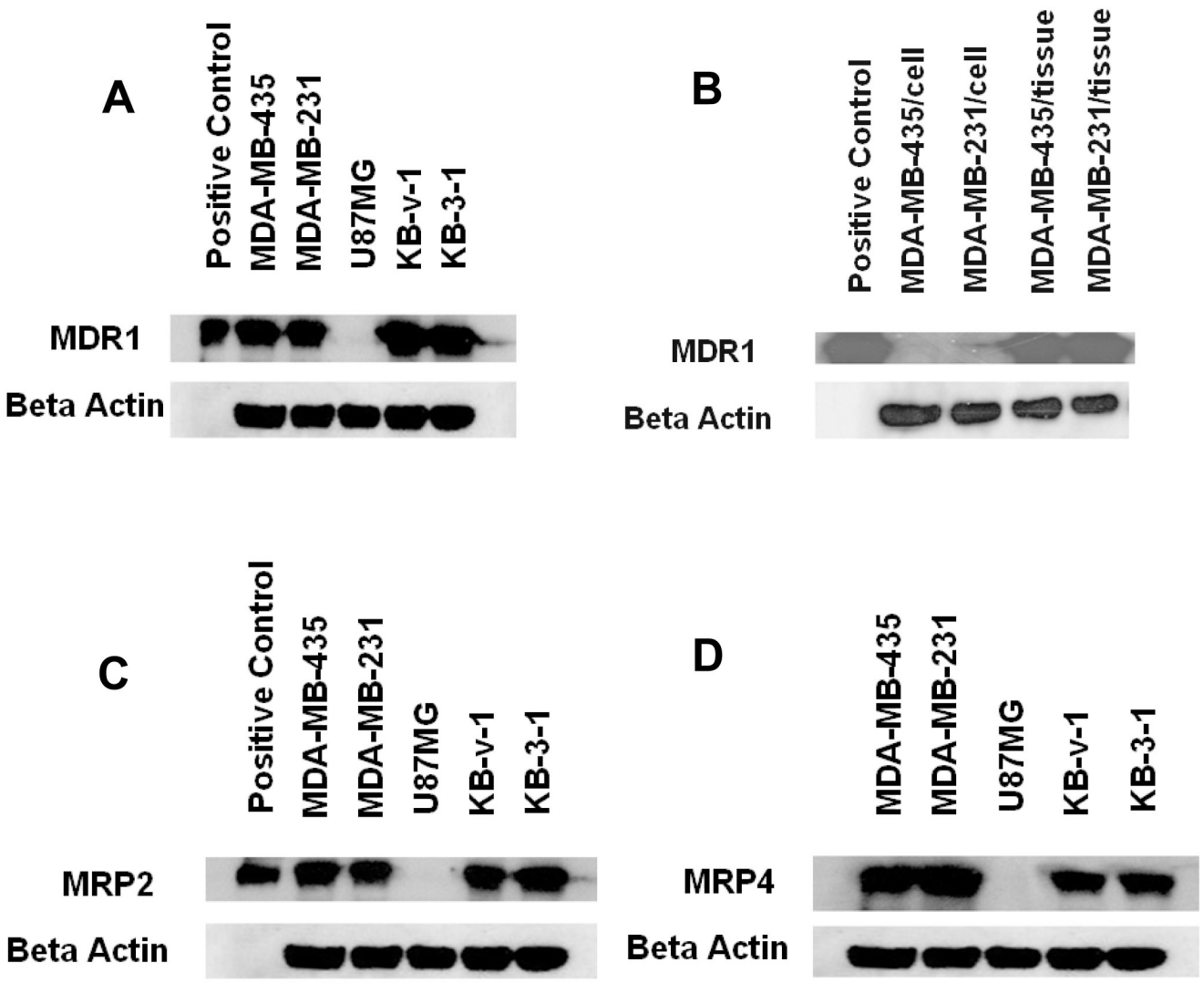

Figure 4.

Western blot data to demonstrate the presence/absence of MDR1 (**A** and **B**), MRP2 (**C**) and MRP4 (**D**) in U87MG (MDR1, MRP2 and MRP4-negative), MDA-MB-435 (MDR1-negative in tumor cells but MDR1-positive in tumor tissue, MRP2 and MRP4-positive), MDA-MB-231 (MDR1-negative in tumor cells but MDR1-positive in tumor tissue, MRP2 and MRP4-positive), KB-v-1 and KB-3-1 (MDR1, MRP2 and MRP4-positive).

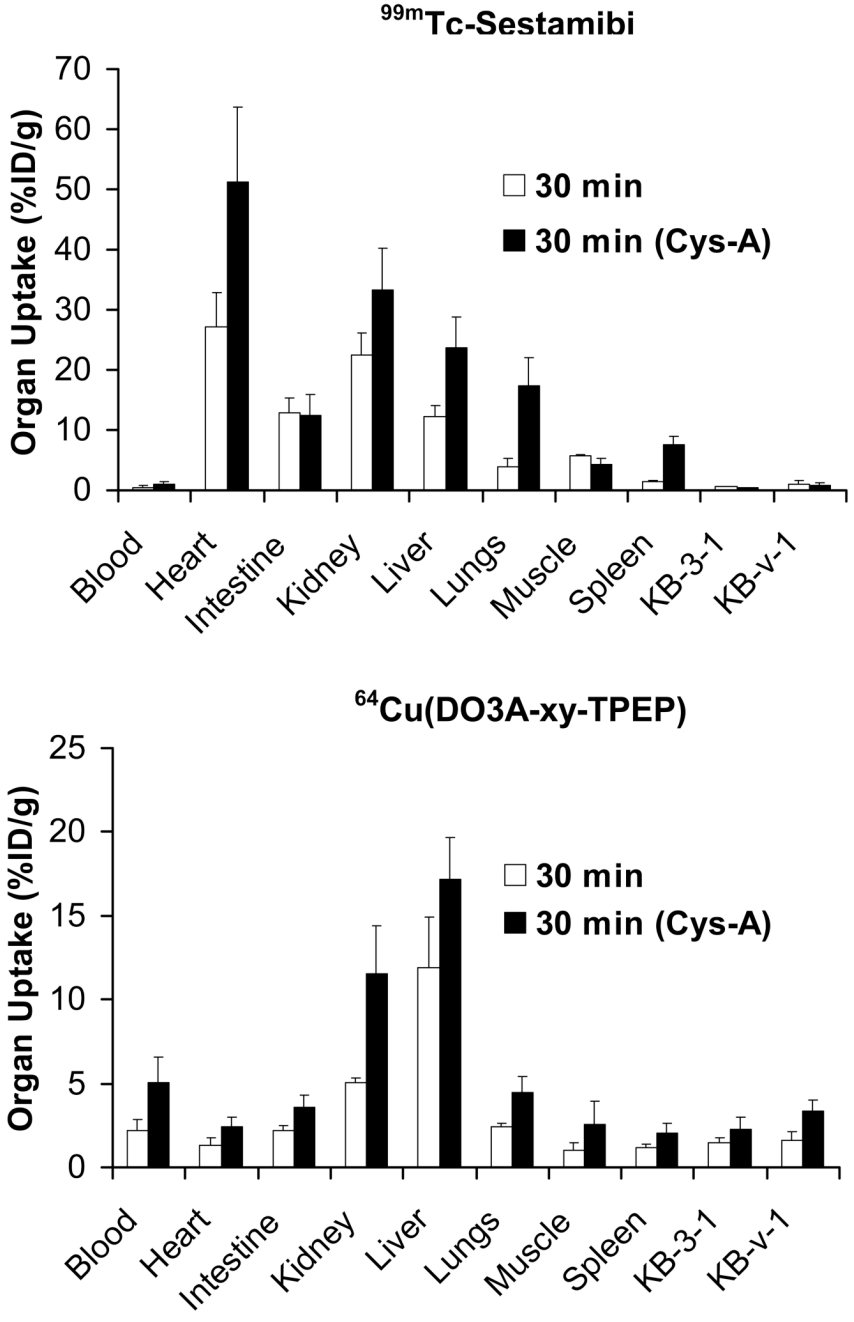

Figure 5.
Impact of Cys-A on the uptake of ^{64}Cu(DO3A-xy-TPEP) and ^{99m}Tc-Sestamibi in selected organs of the athymic nude mice bearing KB-v-1 and KB-3-1 tumor xenografts.

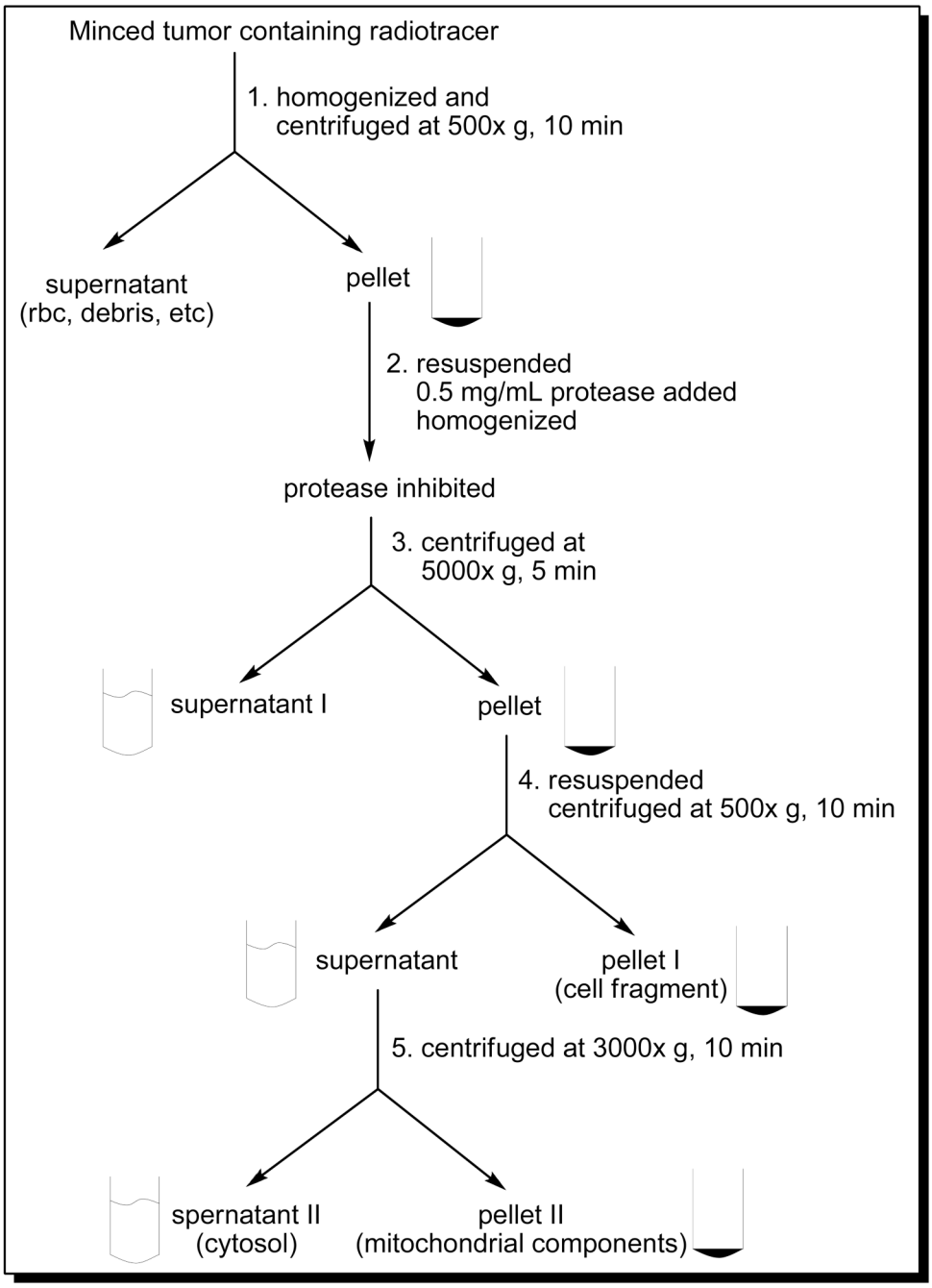

Figure 6.
Schematic presentation of the standard differential centrifugation process.

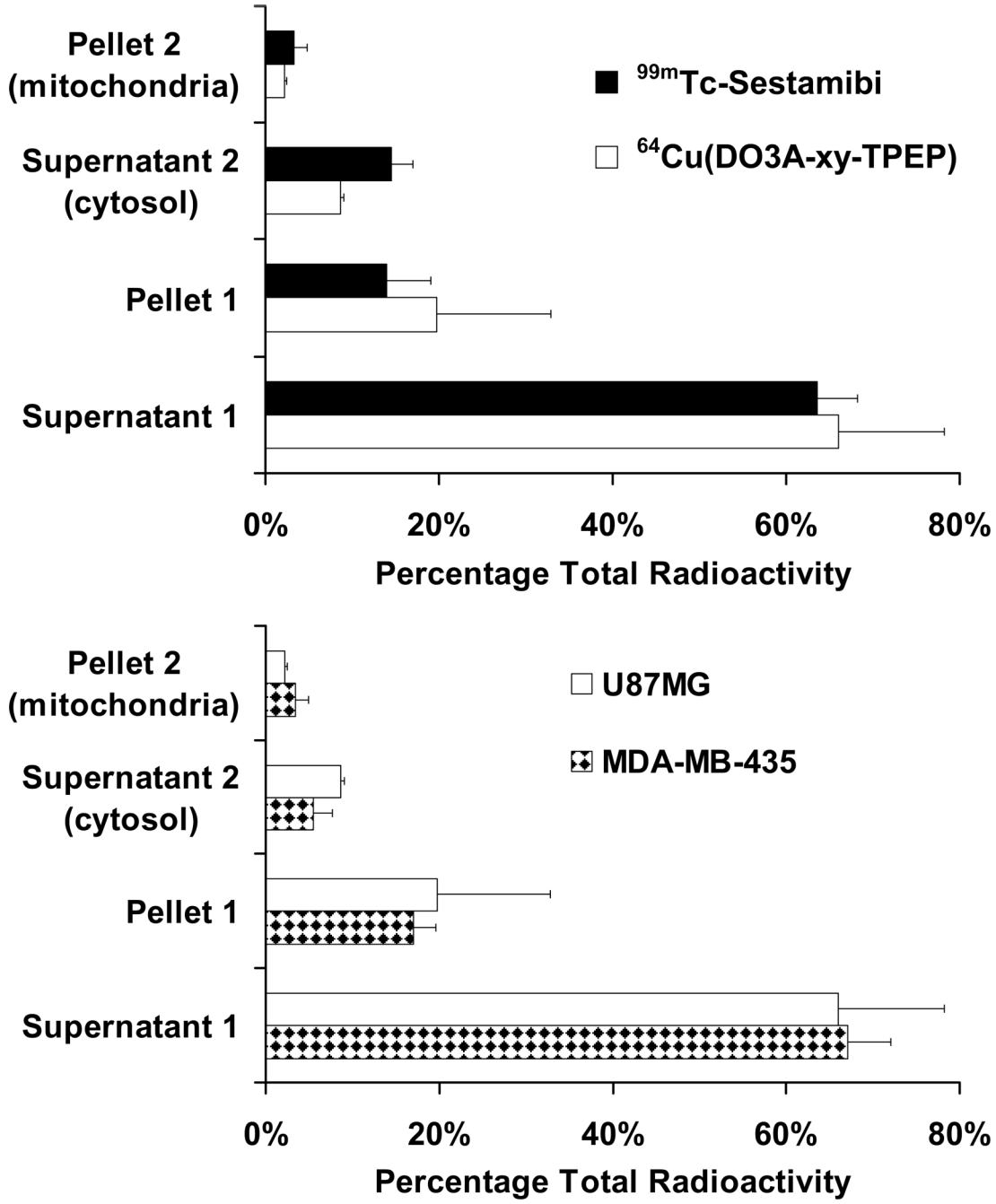

Figure 7.
Top: subcellular distribution properties of ^{64}Cu(DO3A-xy-TPEP) and ^{99m}Tc-Sestamibi in U87MG human glioma xenografts; Bottom: direct comparison of subcellular distribution patterns of ^{64}Cu(DO3A-xy-TPEP) in the U87MG glioma and MDA-MB-435 breast tumor xenografts.

Table 1

Biodistribution data for ^{64}Cu(DO3A-xy-TPEP) in xenografted tumor-bearing athymic nude mice. The tumor uptake is reported as an average ± standard deviation based on the results from three tumor-bearing mice, unless specified, at each time point. The normal organ uptake values are reported as an average ± standard deviation based on the results from fifteen tumor-bearing mice (3 animals for each tumor type, and a total of five different tumor types) at each time point.

Organ	5 min	30 min	60 min	120 min
Blood	9.52 ± 1.19 (n = 9)	2.09 ± 0.90 (n = 15)	1.30 ± 1.10 (n = 15)	0.84 ± 0.62 (n = 15)
Brain	0.22 ± 0.06 (n = 9)	0.10 ± 0.09 (n = 15)	0.06 ± 0.05 (n = 15)	0.02 ± 0.02 (n = 15)
Heart	4.04 ± 0.70 (n = 9)	1.25 ± 0.48 (n = 15)	0.92 ± 0.43 (n = 15)	0.55 ± 0.09 (n = 15)
Intestine	4.06 ± 0.78 (n = 9)	3.23 ± 1.22 (n = 15)	2.87 ± 1.28 (n = 15)	2.61 ± 1.26 (n = 15)
Kidney	31.79 ± 8.02 (n = 9)	6.77 ± 1.63 (n = 15)	4.11 ± 1.11 (n = 15)	2.98 ± 0.53 (n = 15)
Liver	8.03 ± 1.33 (n = 9)	8.74 ± 3.30 (n = 15)	8.66 ± 4.85 (n = 15)	5.59 ± 1.39 (n = 15)
Lungs	7.72 ± 0.74 (n = 9)	2.50 ± 0.61 (n = 15)	2.19 ± 0.91 (n = 15)	1.51 ± 0.18 (n = 15)
Muscle	3.07 ± 0.45 (n = 9)	0.82 ± 0.39 (n = 15)	0.81 ± 0.98 (n = 15)	0.10 ± 0.06 (n = 15)
Spleen	2.73 ± 0.31 (n = 9)	1.14 ± 0.37 (n = 15)	0.84 ± 0.40 (n = 15)	0.56 ± 0.17 (n = 15)
U87MG	5.27 ± 0.99 (n = 3)	2.09 ± 0.53 (n = 3)	2.58 ± 0.31 (n = 3)	3.35 ± 1.27 (n = 3)
MDA-MB-435	2.73 ± 0.55 (n = 3)	1.05 ± 0.19 (n = 3)	1.12 ± 0.20 (n = 3)	0.81 ± 0.11 (n = 3)
MDA-MB-231	3.54 ± 0.15 (n = 3)	1.57 ± 0.04 (n = 3)	1.10 ± 0.17 (n = 3)	0.93 ± 0.15 (n = 3)
KB-v-1		2.00 ± 0.48 (n = 6)	1.58 ± 0.47 (n = 6)	0.93 ± 0.22 (n = 3)
KB-3-1		1.97 ± 0.61 (n = 6)	1.46 ± 0.26 (n = 6)	1.16 ± 0.19 (n = 3)

Table 2

Biodistribution data for ^{99m}Tc-Sestamibi in xenografted tumor-bearing athymic nude mice. The tumor uptake is reported as an average ± standard deviation based on the results from three tumorbearing mice at each time point, unless specified. The normal organ uptake values are reported as an average ± standard deviation based on the results from nine tumor-bearing mice (3 animals for each tumor type, and a total of three different tumor types) at each time point.

Organ	5 min	30 min	60 min	120 min
Blood	0.87 ± 0.44 (n = 6)	0.26 ± 0.28 (n = 9)	0.28 ± 0.34 (n = 9)	0.08 ± 0.03 (n = 9)
Brain	0.22 ± 0.05 (n = 6)	0.15 ± 0.05 (n = 9)	0.11 ± 0.02 (n = 9)	0.08 ± 0.02 (n = 9)
Heart	19.22 ± 6.96 (n = 6)	20.52 ± 1.11 (n = 9)	20.07 ± 3.99 (n = 9)	20.88 ± 4.55 (n = 9)
Intestine	9.80 ± 2.74 (n = 6)	11.13 ± 1.62 (n = 9)	11.11 ± 4.54 (n = 9)	5.29 ± 2.52 (n = 9)
Kidney	37.45 ± 12.0 (n = 6)	25.50 ± 5.56 (n = 9)	20.24 ± 4.59 (n = 9)	12.47 ± 3.90 (n = 9)
Liver	14.37 ± 0.92 (n = 6)	9.82 ± 2.12 (n = 9)	8.37 ± 1.90 (n = 9)	5.40 ± 0.42 (n = 9)
Lungs	6.20 ± 2.36 (n = 6)	3.03 ± 1.04 (n = 9)	2.17 ± 0.80 (n = 9)	1.72 ± 0.47 (n = 9)
Muscle	4.84 ± 1.12 (n = 6)	5.02 ± 1.01 (n = 9)	5.25 ± 1.67 (n = 9)	5.22 ± 1.22 (n = 9)
Spleen	3.21 ± 1.27 (n = 6)	1.77 ± 0.554 (n = 9)	1.32 ± 0.33 (n = 9)	1.32 ± 0.90 (n = 9)
U87MG	3.06 ± 0.94 (n = 3)	2.11 ± 0.38 (n = 3)	1.47 ± 0.54 (n = 3)	1.55 ± 0.36 (n = 3)
MDA-MB-435	1.18 ± 0.17 (n = 3)	1.09 ± 0.20 (n = 3)	0.96 ± 0.42 (n = 3)	0.94 ± 0.21 (n = 3)
KB-v-1		0.92 ± 0.61 (n = 3)	1.05 ± 0.86 (n = 3)	0.95 ± 0.47 (n = 3)
KB-3-1		0.53 ± 0.09 (n = 3)	0.31 ± 0.09 (n = 3)	0.22 ± 0.03 (n = 3)